Accepted manuscript of article: Cisneros, J., Best, J., van Dijk, T. et al. Dunes in the world's big rivers are characterized by low-angle lee-side slopes and a complex shape. Nat. Geosci. 13, 156–162 (2020). https://doi.org/10.1038/s41561-019-0511-7

The Shape of Dunes in the World's Big Rivers

Julia Cisneros[1,*], Jim Best[1,2], Thaienne van Dijk[3], Renato Paes de Almeida[4,5], Mario Amsler[6], Justin Boldt[7], Bernardo Frietas[8], Cristiano Galeazzi[4], Rick Huizinga[9], Marco Ianniruberto[10], Hongbo Ma[11], Jeff Nittrouer[11], Kevin Oberg[12], Oscar Orfeo[13], Dan Parsons[14], Ricardo Szupiany[15], Ping Wang[16], and Yuanfeng Zhang[16]

[1]University of Illinois at Urbana Champaign, Department of Geology, Urbana, IL, USA
[2]University of Illinois at Urbana Champaign, Departments of Geography & GIS, Mechanical Science and Engineering and Ven Te Chow Hydrosystems Laboratory, Urbana, IL, USA
[3]Deltares, Department of Applied Geology and Geophysics, Utrecht, The Netherlands
[4]Instituto de Geociências, Universidade de São Paulo, São Paulo, SP, Brazil
[5]Instituto de Energia e Ambiente, Universidade de São Paulo, São Paulo, Brazil
[6]Instituto Nacional de Limnologia (INALI-CONICET-UNL), Ciudad Universitaria, Santa Fe, Argentina.
[7]USGS Indiana-Kentucky Water Science Center, U.S. Geological Survey, USA
[8]Faculdade de Tecnologia, Universidade Estadual de Campinas, Limeira, SP, Brazil
[9]Missouri Water Science Center, U.S. Geological Survey, USA
[10]Instituto de Geociências, Universidade de Brasília, Brasília, DF, Brazil
[11]Department of Earth, Environmental and Planetary Sciences, Rice University, Houston, TX, USA
[12]Central Midwest Water Science Center, U.S. Geological Survey, USA
[13]National Scientific and Technical Research Council, Centro de Ecología Aplicada, Corrientes, Argentina
[14]University of Hull, Department of Geography, Environment and Earth Sciences, Hull, UK
[15]Faculty of Engineering and Water Sciences, Littoral National University, Santa Fe, Argentina
[16]Yellow River Institute of Hydraulic Research, Zhengzhou, China
[*]Corresponding author: jcisnrs2@illinois.edu
[+]these authors contributed equally to this work

ABSTRACT

Dunes are present in all the worlds' big rivers and form critical agents of bedload transport, constitute appreciable sources of bed roughness and flow resistance, and generate stratification that is the most common depositional element of ancient alluvium. Yet our current models of dunes are conditioned by the geometry of bedforms observed in small rivers and laboratory experiments, and in which the downstream leeside angle is often assumed to be at the angle-of-repose. Here we show, using high-resolution bathymetry from a range of the worlds great rivers, that dunes are instead characterized predominantly by low-angle leeside slopes (<10°), complex leeside shapes where the steepest portion is near the base of the leeside slope, a mean wavelength:height ratio greater than 100, and a height that is often only 10% of the local flow depth. This radically different shape of dunes in the world's big rivers demands that we incorporate such geometries into predictions of flow resistance and water levels, rethink the scaling relationship of dunes when reconstructing alluvial palaeoflow depths, and calls for a fundamental reappraisal of the character, and origin, of low-angle cross-stratification within ancient alluvial sediments.

Introduction

Dunes are a ubiquitous morphological element in all rivers that possess bed material grain sizes ranging from sands to gravels[1], and through their topographic steering of flow are a major source of turbulence within rivers[2]. Sediment transport associated with dunes occurs through dune migration[1,3–5] and by sediment suspension linked to large-scale, dune-related, turbulence. In addition, larger alluvial barforms are created by dune migration and amalgamation, to form areas of hydraulic[1,6], sedimentary[7,8] and ecological[9,10] heterogeneity within a river, which exert a major control on the location of erosion and deposition and the habitat functioning of river beds. As such, dunes exert a major influence on a range of riverine processes, from grain transport to large-scale channel planform change[3,11–13].

Our understanding of the fluid dynamics and sediment transport characteristics of alluvial dunes has been guided largely by the study of small dunes in both the laboratory and field[14–17], with only a few studies having examined flow over dunes in big rivers where dunes with leesides less than the angle-of-repose are present[18–21], and where multiple scales of bedform interact to create complex dune shapes[6,12,22,23]. Research has also shown that dunes with more complex shaped leeside slopes

possess a different flow dynamics to dunes with high-angle, simple leesides[1,19,21,24]. Specifically, low-angle dunes (defined herein as dunes with a leeside angle less than 10°), do not possess a zone of permanent flow separation, and dunes with leeside angles less than 4° have been argued to not exhibit flow separation at all[21,24–28], which consequently causes lower energy losses arising from turbulent eddy shedding in the shear layer between the recirculating flow in the dune leeside and overlying free flow[1]. Furthermore, a scaling relationship between formative flow depth and dune height is often assumed when predicting dune dimensions in modern channels, and reconstructing dune size and flow depth in paleohydraulic reconstructions of ancient riverine sediments[8,16,29–31]. However, recent work[32] has re-evaluated such dune scaling relationships by compiling data from both laboratory and field datasets (~50) and concluded that there is a change in dune morphology from an asymmetric to a more symmetric shape and from high to lower angle leesides in shallow (<2.5 m) and deep flows, respectively. This has been attributed to a likely change in the dominant processes controlling dune formation as dunes become larger, and thus different scaling relationships have been suggested for shallow and deep flows[32].

However, we presently lack a detailed quantification of the morphology of dunes within large alluvial channels in order to assess exactly what shape of dunes are most common in the world's biggest rivers, and thereby assess the potential importance of dune shape in predicting the behavior of modern rivers and reconstructing the paleohydraulics of ancient fluvial channels. Here, we present and analyze a unique dataset that permits quantification of the shape of dunes in six of the world's major rivers - the Amazon, Mekong, Mississippi, Missouri, Paraná and Waal rivers. This analysis reveals the dominance of low-angle dunes with a complex leeside shape, and highlights that current models of dunes in modern and ancient sediments must better recognize and incorporate the fundamental geometry of these ubiquitous morphological elements.

Methods and Field Data

Field data from six of the world's major rivers, the Amazon, Mekong, Mississippi, Missouri, Paraná and Waal rivers, were acquired using a multi-beam echosounder (MBES). During data acquisition, a MBES is attached to a moving vessel and multiple (up to 512) acoustic beams are transmitted through the water column to the river bed, thus forming a beam swath as the boat traverses the river. The travel time of the signal from the MBES transmitter to the riverbed and back to the receiver is used to calculate the water depth given a simultaneous measurement of the acoustic velocity in water. The position of the vessel is resolved via a Differential Global Positioning System (DGPS) and an inertial motion unit to correct for pitch, roll and heave, thus yielding bathymetric measurements of centimetric resolution in the x,y, and z components. The MBES surveys reported herein (see Supplementary Figure 1) range in their spatial extent between 0.1 km^2 (Missouri River) - 6 km^2 (Amazon River) and survey acquisition time ranged from one day (Missouri River) to three days (Amazon River) depending on survey extent and field conditions. A bedform analysis method for bathymetric information (BAMBI) was developed and applied to the MBES data and quantified the shape of dunes in each river (see Supplementary Methods). Shape descriptors of each dune include dune height, wavelength, average leeside angle, maximum slope angle on the leeside, and the location of the maximum slope, as well as flow depth at each dune. From the MBES data, bedforms are measured across the width of the entire survey area at spanwise steps equal to the MBES grid resolution (0.5 m in all cases), and so in this way one dune will be measured across its entire width. In addition to MBES data, dune shapes from data acquired by a single echosounder system in the Huang He (Yellow) River measured using the BAMBI method and dune data measured by hand from single beam echo sounder surveys of the Jamuna (Brahmaputra) River[18] are presented (Table S1 and Supplementary Figures 2 and 3) as additional data for comparison to dune leeside angles quantified from MBES data.

Dune Leeside Angle and Shape

Histograms of mean leeside angle possess a peak at *c.* 10° (peaks range 10.2-16.1°; Figure 1a-f), an average standard deviation of 5.72°, and are skewed (about 1.4° on average) towards lower leeside values, with 48 to 90% of the dunes in each river possessing leeside slopes less than 15° (see Table S1). Single echosounder lines (Supplementary Figures 2 and 3) also reveal a similar relation in the Jamuna River[18] (n = 770), where dune leeside angles were on average 10.2°, and in the Huang He River where dunes have a mean leeside angle of *c.* 2.0° (n = 97). The histograms of maximum leeside angle show peaks around 20° (Figure 1h-m), with the histogram shapes having a larger standard deviation about the mean, ranging from 5.5 to 9.9°, and with 31% of leeside angles, on average, being between 20 and 30° (see Table S1).

Plotting this unique dataset for mean and maximum leeside angle in big rivers in one histogram shows a good fit to a gamma relationship rather than a normal fit (Figure 1g), confirming previous research that a positively skewed probability density function is the best representation of dune morphologic data[33]. The average mean and maximum leeside angles are 13.4° and 20.5°, respectively. The composite histogram of mean leeside angle reveals that 75.4% of all dunes measured herein possess leeside angles less than 15°. For the composite histogram of maximum leeside angle, a peak is present at 20.5°, with maximum leeside angles ranging from 10 - 30°, and with 25.2% of all leesides being between 20-30° (refer to shaded area in Figure 1). These higher values are more representative of traditional angle-of-repose leeside dune slopes, although it is important to highlight that this value of maximum angle only represents a singular maximum slope on the entire leeside, whereas the mean angle represents the average of all slopes on the leeside.

The overlaps between the histograms of mean and maximum leeside angle suggest that the singular high slope values reported in the maximum leeside histogram are not representative of the entire leeside slope. Thus, the position of the maximum leeside angle along the leeside slope is critical, since these steeper slopes will influence the flow dynamics, and especially the production of flow separation, in the dune leeside that is instrumental to flow resistance and energy loss associated with the dune. The present data uniquely allow the position of the maximum leeside slope to be quantified, and is expressed herein as the height of the maximum leeside slope, h, with respect to the total dune height, H, from the base of the leeslope (Figure 2a). This data (Figure 2b) shows that the position of the maximum leeside slope is dominantly at 0.3-0.4 h/H (i.e. in the bottom half of the leeside slope) and the distribution is slightly shifted towards lower values, such that the maximum leeside slope is more commonly located <0.5 h/H (Figure 2b). These results thus demonstrate that even if the leeside is gently sloping at a mean of 10°, a maximum slope of 20° could be present on the dune leeside but would most likely be located towards the bottom half of the leeside. Importantly, the occurrence of higher angle slopes towards the base of the leeside will be far less influential in creating significant flow separation than if they were present at the top of the leeside slope.

Dune Size and Potential for Flow Separation

Dune height (H) plotted against flow depth (Y) for each river (Figure 3) shows that in flow depths less than *c.* 5 meters, H=0.33Y represents the upper limit of dune height, but for all flow depths 82 % of all dunes fall below the H=0.10Y relation (see Table S2). In flow depths greater than 30 meters, 96% of dunes have heights at, or below, 5 meters (<0.167Y). While dunes with heights up to 10 meters do exist in deep flows, such as those in the Amazon River, smaller dunes (H<0.10Y) are much more common in such deep channels. This fact challenges the often made assumption that bigger rivers must be characterized by larger dunes. In addition, the wavelength:height ratio of dunes (Supplementary Figure 4) shows a wide range (mean values for individual rivers range from 69-170), with a mean and standard deviation for all rivers of 133 and 315 respectively.

The size of the flow separation zone in the dune leeside may be considered a function of dune height in relation to flow depth (that determines flow velocity at the crest), leeside slope angle and additionally the location of the maximum leeside slope. Plotting mean dune leeside angle against the submerged dune height (H/Y; Figure 4) for maximum leeside angles located in the top and bottom half of the dune height (Figs 4a and 4b respectively) allows consideration of the potential for flow separation associated with dunes in the world's big rivers. In addition, Figure 4 uses past experimental data to highlight: i) dunes where permanent flow separation is absent (leeside angles below 10°[21,24–28]), ii) the onset of permanent flow separation, which is dependent on H/Y and occurs over a range of leeside angles (defined here by a linear interpolation between three experimental test cases[27]), and iii) where fully developed flow separation is present and associated with dunes that possess leeside angles greater than 24°[27]. The majority (93.8 %) of dunes with maximum leeside angles between 11-18° fall below the experimentally derived line where the onset of permanent flow separation has been observed, and only a very low percentage of dunes (<1%) exhibit permanent flow separation (Fig. 4). For dunes with leeside slopes less than 10°, where there is likely no permanent flow separation, the maximum slopes are more common in the lower part of the dune leeside (44%) than in dunes with maximum slopes located in the upper part of the leeside (36%).

This unique dataset thus illustrates that the overwhelming majority of dunes in the world's big rivers have low-angle leesides (mean *c.* 10°) that are significantly less than the angle-of-repose, possess heights (H<0.1Y) far less than commonly assumed with respect to the flow depth, and that even the steeper segments of their leesides occur predominantly towards the bottom of the leeside slope. These morphological characteristics, and their influence on fluid flow, have profound implications for the models of flow required for the most common bedform in the world's large rivers, how flow resistance is predicted and modelled in such channels and how the deposits of such dunes are recognized in ancient alluvial successions.

Discussion

Although low-angle dunes with complex leeside shapes have been documented previously in the Brahmaputra[18], Fraser[20] and Amazon[34,35] rivers, and their flow dynamics has received limited study using physical and numerical models[21,25–28], the present results provide the most comprehensive analysis yet accomplished detailing the morphology of dunes in some of the world's biggest rivers. Our findings reveal the dominance of low-angle dunes and complex dune shapes, with 75% of dunes possessing leeside angles <14.9°. These results demonstrate the ubiquity of such dunes and suggest that it is essential to account for their morphology when both modelling modern rivers and interpreting their deposits in ancient alluvial successions. Three implications arise from these contentions.

First, low-angle dunes will generate less turbulence than classic angle-of-repose dunes[19,27], thereby lessening flow resistance caused by dune form roughness[11,36–38]. Parameterization of such roughness and the nature of flow separation[37,38] associated with low-angle dunes should thus be included in fluid dynamic models of alluvial channels[39], and a composite PDF, such as that presented herein (Figure 1g), provides a desirable quantification in the absence of site-specific data in order to better represent such roughness. The present data also builds on previous work[24] that suggests dune leeside shape is complex, but further quantifies leeside shape by showing that the steepest sections of the leeside are predominantly nearer the leeside base, and not

near the top of the leeface. This again alludes to the lesser role of flow separation, and linked flow resistance, over such leesides. The processes that lead to complex leeside shapes likely revolve around bedform superimposition and amalgamation[12,22,23], the possible influence of sediment in suspension[40], together with the modifications to dune morphology associated with transitional dunes[41,42], all of which may be greatly influenced by spatio-temporal changes in flow during flood hydrographs and the effects of bedform hysteresis[42–46]. Nevertheless, the dominance of dunes with these shapes in large rivers demonstrates their morphology must be reflected in models that seek to predict flow and sediment transport[39], as well as the effects of such dunes on larger scale bar formation and channel development[13].

Secondly, in the ancient alluvial record, dune cross-stratification has often been used to reconstruct flow depths[8,30], and thus help constrain parameters such as channel size and flow discharge[29,31,47], with the relationship between dune height and flow depth being pivotal in such paleohydraulic reconstructions. The present extensive dataset illustrates that, rather than assuming a relationship between flow depth and dune height of $H \cong 0.25 - 0.33Y$ as in much past work[47], it is better to adopt a value of $H \cong 0.1Y$. This value, together with a factor accounting for the preservation of the dune[8,23,35,48], should be adopted to yield more realistic estimates of mean flow depths. This contention thus suggests that many past predictions of alluvial paleoflow depth based on dune height may have been underestimates, and highlights the need to obtain other independent estimates of flow depth where possible, such as from the thickness of channel fill sequences[49] or the height of larger-scale barform-generated stratification[50].

Lastly, the dominance of low-angle dune leesides in the world's large rivers suggests that the recognition, in both outcrop and core, of such dunes in ancient alluvial successions may require that far more attention be devoted to low-angle stratification. Our data illustrate that low leeside angles are very common, with dips of only a few degrees often being present (Figs 1, 4), and thus low-angle stratification, which may appear essentially flat, especially in core, may require greater consideration in its interpretation. Such low-angle surfaces in alluvial successions may be simply the product of low-angle dunes, rather than conditions representative of upper-stage plane bed conditions[41,51]. Where dunes are large, with leesides many meters or tens of meters long, such low-angle stratification may be extremely difficult to recognize in outcrop, and demands careful tracing of individual laminae, and the subtle erosional surfaces between superimposed low-angle dunes. It is also apparent that complex dune leesides, and the presence of multiple scales of dunes, are commonplace in the world's large rivers, and suggests that the key to establishing the scale of a paleoflow and alluvial channel size may lie in interpretations of the smaller, cross-stratified cosets and the erosional surfaces between them[35]. Our work demonstrates that it is essential to recognize the presence, scale and dominance of low-angle complex dunes within the majority of alluvial channels, if we are to better account for their influence on the dynamics of contemporary river channels, and their recognition in ancient alluvial sequences.

Supplementary Methods

Recently, several methods to automate the detection and measurement of bedform morphology have been proposed using geostatistical and signal-processing techniques[52,53]. These methods are often unable to account for complexities in bedform morphology, such as leeside shape, and the data outputs are typically statistical values that represent mathematical fits to the raw data rather than measurements of the raw data. In addition, most methods only focus on analyzing bedforms taken from a limited number of profile lines and, whilst a few methods can analyze the entire bathymetric bedform field, most of these methods are computationally expensive. Thus, there exists a need for a bedform analysis method that utilizes the raw bathymetric data, treats the bedforms as having a complex morphology, outputs values that represent such complexity, and is computationally efficient and robust. Such a method will be invaluable in quantifying bedform shape from high-resolution bathymetric datasets and allow the user to gain better knowledge of spatially variable bedforms. In the research reported herein, a Bedform Analysis Method for Bathymetric Information (BAMBI) was developed to automatically measure the geometric characteristics of dunes in big rivers using multi-beam echosounder data acquired for several large rivers. The BAMBI can also be used to measure dunes from single echosounder lines, but additional steps must be made so that the lines are in a matrix format as the BAMBI begins by defining each data point as being related to the eight other surrounding points in a 3x3 window. BAMBI works at the resolution of the data and in the present analysis increased data output from a few hundred measurements to over two hundred and fifty thousand data points, whilst also decreasing data measurement time to a few hours of code run time. Thus, the BAMBI allowed for a highly resolved and spatially extensive analysis herein of six of the worlds big rivers to yield a unique new quantification.

In BAMBI (see Figure S5 for flow chart of methodology), the inputs required are an ASCII file of river bathymetry gathered via multi-beam echosounder, a general downstream estimate of flow direction in azimuthal coordinates of the river, and a flow looking angle (the deviation around the flow direction that defines what is considered a downstream-facing slope; set at default as 40°). In the case that MBES xyz data is not available and single echosounder lines must be used, the lines must be used to construct an artificial matrix. Here the lines, with their georeferenced x,y, locations, must be spaced equally in the x and y directions and stacked in a matrix by groups of three. In this way, the matrix will have three columns of NaN, followed by three columns of the echosounder line repeated, and three more columns of NaN. In addition, all echosounder lines must be

aligned with the flow direction. In the case that echosounder lines are not perfectly straight, the user must decide the best way to interpolate the data onto a straight line. All lines can be placed in the same matrix, as long as packages of three NaN columns straddle each package of three repeated echosounder lines.

The output of the analysis method is a text file of 9 columns: X coordinate (latitude), Y coordinate (longitude), dune height, dune mean leeside angle, dune maximum leeside angle, leeside slope direction, dune wavelength, dune flow depth (taken at the crest), and the fractional height of the maximum slope on the leeside for each dune measured across the river width at steps of the data resolution (herein 0.5 meters). To begin, the raw bathymetric data is rotated so that the grid is aligned with the flow direction oriented to 0°, or in other words, the grid is rotated to $\theta = -\text{flow direction} = 0$. Now, the grid can be analyzed by column, which coincides with individual profile lines in the flow direction. The first step in the analysis method is to create slope and aspect grids from the rotated raw bathymetric depth data by using a 3x3 floating window [a,b,c; d,**e**,f; g,h,i]. This computes slope and aspect for each **e** cell as the window moves through the grid (cellsize equal in x and y) in the following way, where x and y are in a 2D matrix, and z is the third dimension:

$$[dz/dx] = ((c+2f+i)-(a+2d+g)/(8*x_{cellsize}) \tag{1a}$$

$$[dz/dy] = ((g+2h+i)-(a+2b+c))/(8*y_{cellsize}) \tag{1b}$$

$$rise\_run = \sqrt{[dz/dx]^2+[dz/dy]^2} \tag{1c}$$

$$slope\_degrees = ATAN(rise\_run)*57.29578 \tag{1d}$$

$$aspect = 57.29578*ATAN2([dz/dy],-[dz/dx]) \tag{1e}$$

$$\begin{array}{ll} \text{if} & aspect < 0, cell = 90.0 - \text{aspect} \\ \text{else if} & aspect > 90.0, cell = 360.0 - aspect + 90.0 \\ \text{else} & cell = 90.0 - aspect \end{array} \tag{1f}$$

Once the slope and aspect grids are computed, a leeside cell is defined as a cell with aspect direction in the range of the flow direction $\pm$ the flow looking angle. All other cells are defined as stoss cells. Thus, a crest location is where a cell changes from stoss to lee side cell and a trough is where a cell changes from a lee to a stoss side cell. Dune height is then computed as the difference between the crest and the following trough cell depth. The dune mean leeside angle is computed as the average of all consecutive lee cell values in the dune leeside, whilst the maximum leeside angle is taken as the singular, maximum lee cell value in the dune leeside. The fractional height of the maximum leeside angle is then computed as the cell height of the maximum lee cell divided by the entire leeside height (dune height) of the dune. At this point, information is computed for dunes of all scales (i.e. superimposed and larger formative dunes), and thus a bedform threshold is applied that is the mean plus the standard deviation of all dune heights computed within the MBES survey. This is conducted under the assumption that smaller scale bedforms are more common in the river and these values shift the bedform height distribution to be peaked at lower values. Once this threshold is found, all dunes that have heights less than the threshold are saved separately as 'small' dunes. These bedforms commonly represent small, superimposed dunes. The remaining dunes are then assumed to be the larger formative dunes in the river. Once the formative scale dunes have been defined, the dune wavelength is computed as the distance between the troughs that bracket the formative dunes. This is also applied for the separate grid of smaller scale dunes within BAMBI.

References

1. Best, J. L. The fluid dynamics of river dunes: A review and some future research directions. *J. Geophys. Res. Earth Surf.* **110** (2005).

2. Parsons, D. R. *et al.* Form roughness and the absence of secondary flow in a large confluence–diffluence, Rio Paraná, Argentina. *Earth Surf. Process. Landforms* **32**, 155–162 (2007).

3. Allen, J. R. L. The diffusion of grains in the lee of ripples, dunes, and sand deltas. *J. Sedimentary Res.* **38** (1968).

4. Bennett, S. J. & Best, J. L. Mean flow and turbulence structure over fixed, two-dimensional dunes: implications for sediment transport and bedform stability. *Sedimentology* **42**, 491–513 (1995).

5. McLean, S. R., Nelson, J. M. & Wolfe, S. R. Turbulence structure over two-dimensional bed forms: implications for sediment transport. *J. Geophys. Res. Ocean.* **99**, 12729–12747 (1994).

6. Parsons, D. R. *et al.* Morphology and flow fields of three-dimensional dunes, Rio Paraná, Argentina: Results from simultaneous multibeam echo sounding and acoustic Doppler current profiling. *J. Geophys. Res. Earth Surf.* **110** (2005).

7. Jordan, D. W. & Pryor, W. A. Hierarchical levels of heterogeneity in a Mississippi River meander belt and application to reservoir systems: Geologic note (1). *AAPG Bull.* **76**, 1601–1624 (1992).

8. Leclair, S. F. & Bridge, J. S. Quantitative interpretation of sedimentary structures formed by river dunes. *J. Sedimentary Res.* **71**, 713–716 (2001).

9. Amsler, M. L., Blettler, M. C. & Ezcurra de Drago, I. Influence of hydraulic conditions over dunes on the distribution of the benthic macroinvertebrates in a large sand bed river. *Water Resour. Res.* **45** (2009).

10. Allan, J. D. & Castillo, M. M. *Stream ecology: structure and function of running waters* (Springer Science & Business Media, 2007).

11. Einstein, H. A. *The bed-load function for sediment transportation in open channel flows*, vol. 1026 (US Department of Agriculture Washington, DC, 1950).

12. Allen, J. R. L. Polymodal dune assemblages: an interpretation in terms of dune creation—destruction in periodic flows. *Sedimentary Geol.* **20**, 17–28 (1978).

13. Hickin, E. J. The development of meanders in natural river-channels. *Am. J. Sci.* **274**, 414–442 (1974).

14. Southard, J. B. & Boguchwal, L. A. Bed configuration in steady unidirectional water flows; Part 2, Synthesis of flume data. *J. Sedimentary Res.* **60**, 658–679 (1990).

15. Van Den Berg, J. I. & Van Gelder, A. A new bedform stability diagram, with emphasis on the transition of ripples to plane bed in flows over fine sand and silt. *Spec. Publ. Int. Ass. Sediment.* **17**, 11–21 (1993).

16. Yalin, M. S. Geometrical properties of sand wave. *J. Hydraul. Div.* **90**, 105–119 (1964).

17. Guy, H. P., Simons, D. B. & Richardson, E. V. *Summary of alluvial channel data from flume experiments, 1956-61* (US Government Printing Office, 1966).

18. Roden, J. E. *The sedimentology and dynamics of mega-dunes, Jamuna River, Bangladesh*. Ph.D. thesis, University of Leeds (1998).

19. Kostaschuk, R. & Villard, P. Flow and sediment transport over large subaqueous dunes: Fraser River, Canada. *Sedimentology* **43**, 849–863 (1996).

20. Kostaschuk, R. A field study of turbulence and sediment dynamics over subaqueous dunes with flow separation. *Sedimentology* **47**, 519–531 (2000).

21. Best, J. L. & Kostaschuk, R. An experimental study of turbulent flow over a low-angle dune. *J. Geophys. Res. Ocean.* **107** (2002).

22. Allen, J. R. L. & Collinson, J. D. The superimposition and classification of dunes formed by unidirectional aqueous flows. *Sedimentary Geol.* **12**, 169–178 (1974).

23. Reesink, A. J. H. & Bridge, J. S. Influence of superimposed bedforms and flow unsteadiness on formation of cross strata in dunes and unit bars. *Sedimentary Geol.* **202**, 281–296 (2007).

24. Lefebvre, A., Paarlberg, A. J. & Winter, C. Characterising natural bedform morphology and its influence on flow. *Geo-Marine Lett.* **36**, 379–393 (2016).

25. Motamedi, A., Afzalimehr, H., Gallichand, J. & Abadi, E. F. N. Lee angle effects in near bed turbulence: an experimental study on low and sharp angle dunes. *Int. J. Hydraul. Eng.* **1**, 68–74 (2012).

26. Motamedi, A., Afzalimehr, H., Zenz, G. & Galoie, M. RANS simulations of flow over dunes with low lee and sharp lee angles. In *Advances in Hydroinformatics*, 525–533 (Springer, 2014).

27. Lefebvre, A. & Winter, C. Predicting bed form roughness: the influence of lee side angle. *Geo-Marine Lett.* **36**, 121–133 (2016).

28. Kwoll, E., Venditti, J. G., Bradley, R. W. & Winter, C. Flow structure and resistance over subaquaeous high-and low-angle dunes. *J. Geophys. Res. Earth Surf.* **121**, 545–564 (2016).

29. Ashley, G. M. Classification of large-scale subaqueous bedforms: a new look at an old problem-SEPM bedforms and bedding structures. *J. Sedimentary Res.* **60** (1990).

30. Paola, C. & Borgman, L. Reconstructing random topography from preserved stratification. *Sedimentology* **38**, 553–565 (1991).

31. Bridge, J. S. & Tye, R. S. Interpreting the dimensions of ancient fluvial channel bars, channels, and channel belts from wireline-logs and cores. *AAPG bulletin* **84**, 1205–1228 (2000).

32. Bradley, R. W. & Venditti, J. G. Reevaluating dune scaling relations. *Earth-Science Rev.* **165**, 356–376 (2017).

33. Van der Mark, C. F., Blom, A. & Hulscher, S. J. Quantification of variability in bedform geometry. *J. Geophys. Res. Earth Surf.* **113** (2008).

34. de Almeida, R. P. *et al.* Large barchanoid dunes in the Amazon River and the rock record: Implications for interpreting large river systems. *Earth Planet. Sci. Lett.* **454**, 92–102 (2016).

35. Galeazzi, C. P. *et al.* The significance of superimposed dunes in the Amazon River: Implications for how large rivers are identified in the rock record. *Sedimentology* **65**, 2388–2403 (2018).

36. van Rijn, L. C. Sediment transport, Part III: bed forms and alluvial roughness. *J. Hydraul. Eng.* **110**, 1733–1754 (1984).

37. Paarlberg, A. J., Dohmen-Janssen, C., Hulscher, S. & Termes, P. A parameterization of flow separation over subaqueous dunes. *Water Resour. Res.* **43**, W12417 (2007).

38. Paarlberg, A. J., Dohmen-Janssen, C., Hulscher, S. & Termes, P. Modeling river dune evolution using a parameterization of flow separation. *J. Geophys. Res. Earth Surf.* **114**, F01014 (2009).

39. DELTARES. User Manual Delft3D-Flow. *DELTARES, Sep* (2011).

40. Bridge, J. S. & Best, J. L. Flow, sediment transport and bedform dynamics over the transition from dunes to upper-stage plane beds: implications for the formation of planar laminae. *Sedimentology* **35**, 753–763 (1988).

41. Naqshband, S., Ribberink, J. S. & Hulscher, S. J. Using both free surface effect and sediment transport mode parameters in defining the morphology of river dunes and their evolution to upper stage plane beds. *J. Hydraul. Eng.* **140**, 06014010 (2014).

42. Reesink, A. J. *et al.* The adaptation of dunes to changes in river flow. *Earth-Science Rev.* (2018).

43. Ten Brinke, W. B., Wilbers, A. W. & Wesseling, C. Dune growth, decay and migration rates during a large-magnitude flood at a sand and mixed sand–gravel bed in the Dutch Rhine River System. *Fluvial Sedimentol. VI* 15–32 (1999).

44. Wilbers, A. W. & Ten Brinke, W. B. The response of subaqueous dunes to floods in sand and gravel bed reaches of the Dutch Rhine. *Sedimentology* **50**, 1013–1034 (2003).

45. Julien, P. Y., Klaassen, G. J., Ten Brinke, W. B. & Wilbers, A. W. Case study: Bed resistance of Rhine River during 1998 flood. *J. Hydraul. Eng.* **128**, 1042–1050 (2002).

46. Paarlberg, A. J., Dohmen-Janssen, C., Hulscher, S., Termes, P. & Schielen, R. Modelling the effect of time-dependent river dune evolution on bed roughness and stage. *Earth Surf. Process. Landforms* **35**, 1854–1866 (2010).

47. Wignall, P. B. & Best, J. L. The Western Irish Namurian Basin reassessed. *Basin Res.* **12**, 59–78 (2000).

48. Sambrook Smith, G. H., Best, J. L., Orfeo, O., Vardy, M. E. & Zinger, J. A. Decimeter-scale in situ mapping of modern cross-bedded dune deposits using parametric echo sounding: A new method for linking river processes and their deposits. *Geophys. Res. Lett.* **40**, 3883–3887 (2013).

49. Leeder, M. R. Fluviatile fining-upwards cycles and the magnitude of palaeochannels. *Geol. Mag.* **110**, 265–276 (1973).

50. Sambrook Smith, G. H., Ashworth, P. J., Best, J. L., Woodward, J. & Simpson, C. J. The sedimentology and alluvial architecture of the sandy braided South Saskatchewan River, Canada. *Sedimentology* **53**, 413–434 (2006).

51. Best, J. & Bridge, J. The morphology and dynamics of low amplitude bedwaves upon upper stage plane beds and the preservation of planar laminae. *Sedimentology* **39**, 737–752 (1992).

52. van Dijk, T. A., Lindenbergh, R. C. & Egberts, P. J. Separating bathymetric data representing multiscale rhythmic bed forms: A geostatistical and spectral method compared. *J. Geophys. Res. Earth Surf.* **113** (2008).

53. Gutierrez, R. R., Abad, J. D., Parsons, D. R. & Best, J. L. Discrimination of bed form scales using robust spline filters and wavelet transforms: methods and application to synthetic signals and bed forms of the Río Paraná, Argentina. *J. Geophys. Res. Earth Surf.* **118**, 1400–1418 (2013).

Acknowledgements (not compulsory)

JC is supported by National Science Foundation Graduate Research Fellowship (NSF GRF). This material is based upon work supported by the National Science Foundation Graduate Research Fellowship under Grant No. DGE - 1746047. Any opinion, findings, and conclusions or recommendations expressed in this material are those of the author(s) and do not necessarily reflect the views of the National Science Foundation. J.C. is also supported by the Department of Geology, University of Illinois, and the Jack and Richard C. Threet chair to J.B. Other acknowledgements to grant for MBES info from anybody?.

Author contributions statement

J.C. and J.B. conceived the study and identified the potential datasets to be analyzed. J.C. developed the BAMBI code from initial conceptual ideas of J.B., and conducted the analysis and data plotting. All authors provided bathymetric data. J.C., J.B. and T.vD. wrote the initial manuscript that was then reviewed and edited by all authors.

Additional information

To include, in this order: **Accession codes** (where applicable); **Competing financial interests** (mandatory statement).

The corresponding author is responsible for submitting a competing financial interests statement on behalf of all authors of the paper. This statement must be included in the submitted article file.

		N total	Mean	Standard Deviation	Variance	Skewness	Kurtosis	P90	P95	Less than 15° (%)	Between 20 & 30° (%)
Amazon	Mean Lee	15244	10.20	4.94	24.37	3.52	22.25	14.69	17.10	90.84	
	Max Lee	15244	16.45	6.63	43.90	1.91	8.45	23.42	26.60		20.70
Mekong	Mean Lee	53648	12.82	7.51	56.46	1.17	2.46	22.79	26.60	66.49	
	Max Lee	53648	21.06	9.91	98.20	0.33	0.04	33.54	36.29		33.35
Mississippi	Mean Lee	26934	16.10	6.91	47.81	1.00	2.06	24.92	28.52	48.74	
	Max Lee	26934	22.76	7.38	54.45	0.62	1.32	31.74	35.29		48.98
Missouri	Mean Lee	4530	13.65	4.96	24.62	0.33	-0.30	20.20	21.84	59.80	
	Max Lee	4530	18.43	6.08	36.95	0.38	-0.47	27.04	29.06		33.66
Paraná	Mean Lee	39917	13.53	5.84	34.10	1.08	2.40	21.09	24.22	65.58	
	Max Lee	39917	19.90	7.19	51.73	0.49	0.21	29.52	32.39		37.03
Waal	Mean Lee	124836	10.69	4.17	17.41	1.26	7.10	15.85	17.97	86.86	
	Max Lee	124836	14.77	5.55	30.82	1.29	4.53	22.25	26.06		13.12
Average	Mean Lee	–	12.83	5.72	34.13	1.39	6.00	19.92	22.71	69.72	
	Max Lee	–	18.89	7.12	52.68	0.84	2.35	27.92	30.95		31.14
All compiled data	Mean Lee	265109	12.12	5.89	34.66	1.48	4.71	19.65	22.96	75.43	
	Max Lee	265109	17.79	7.78	60.60	0.95	1.54	28.68	32.08		25.24
Jamuna	Mean Lee	770	10.20	16.56	–	–	–	–	–	–	–
	Max Lee	–	–	–	–	–	–	–	–	–	–
Huang He	Mean Lee	97	2.02	1.48	–	–	–	–	–	–	–
	Max Lee	97	4.03	3.00	–	–	–	–	–	–	–

Table S1. Statistics for mean and maximum leesides in each river and all rivers compiled

	N total	Dune height < 0.1Y (%)
Amazon	15244	98.58
Mekong	53648	88.83
Mississippi	26934	91.52
Missouri	4530	39.85
Paraná	39917	63.69
Waal	124836	84.27
Average	44185	77.79
All compiled data	140273	82.89

Table S2. Percentage of dunes with heights that are less than 1/10 flow depth

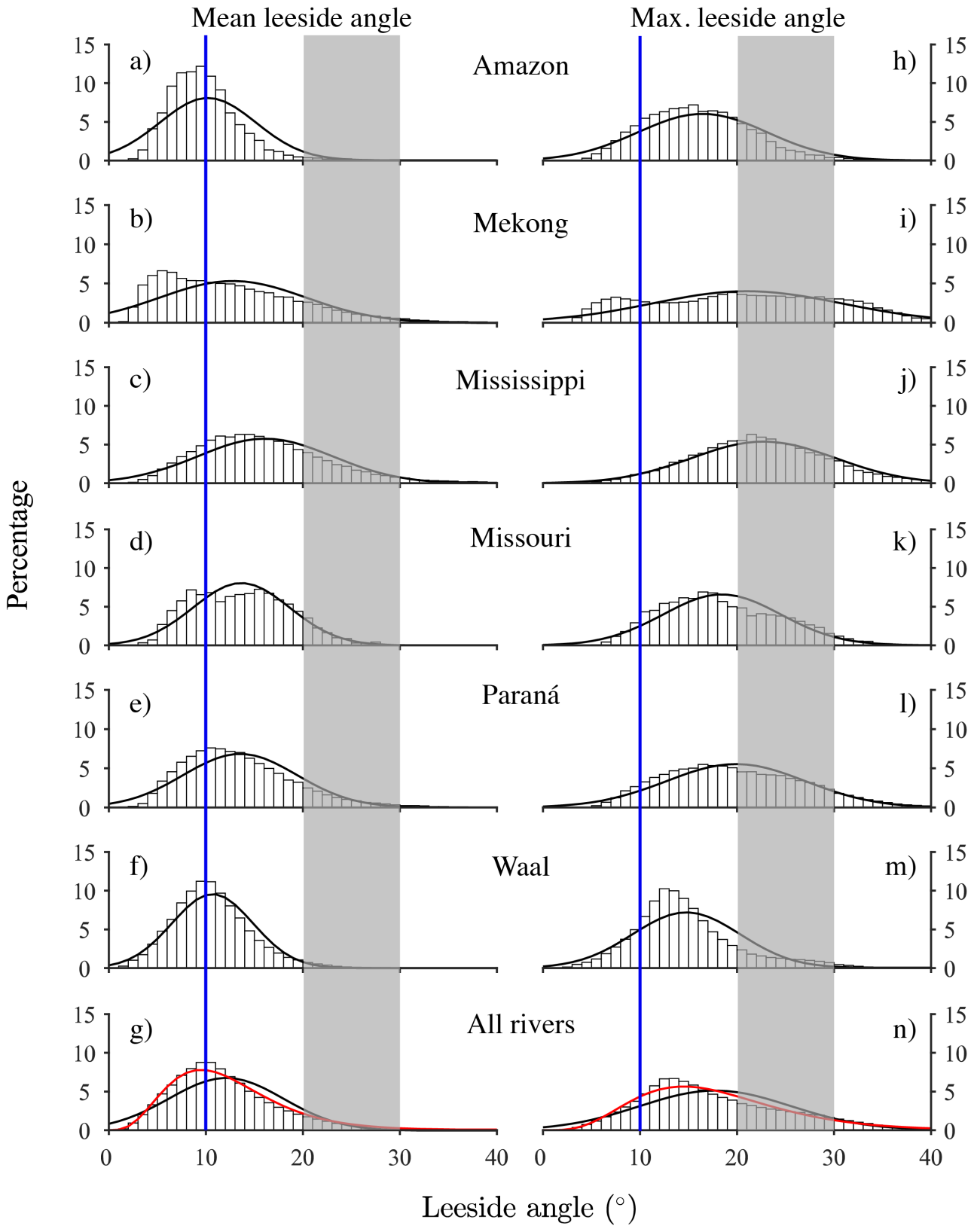

Figure 1. Probability density function (PDF) for mean and maximum dune leeside angles in each river and all rivers combined. Black lines represent normal distribution fits and the red line represents a gamma distribution. The blue line marks leeside angles at 10° and the shaded area highlights leeside angles from 20-30°.

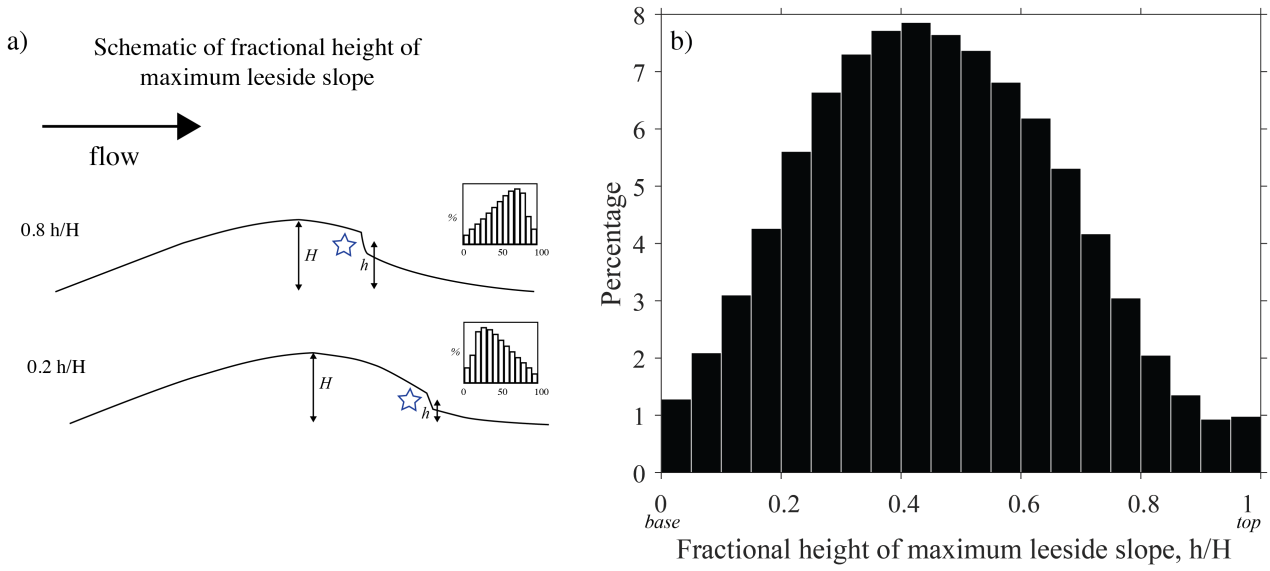

Figure 2. a) Schematic showing the location of a maximum slope at 0.2 and 0.8 H for a dune profile. b) PDF of the fractional height of the maximum slope angle on the dune leeside for all rivers.

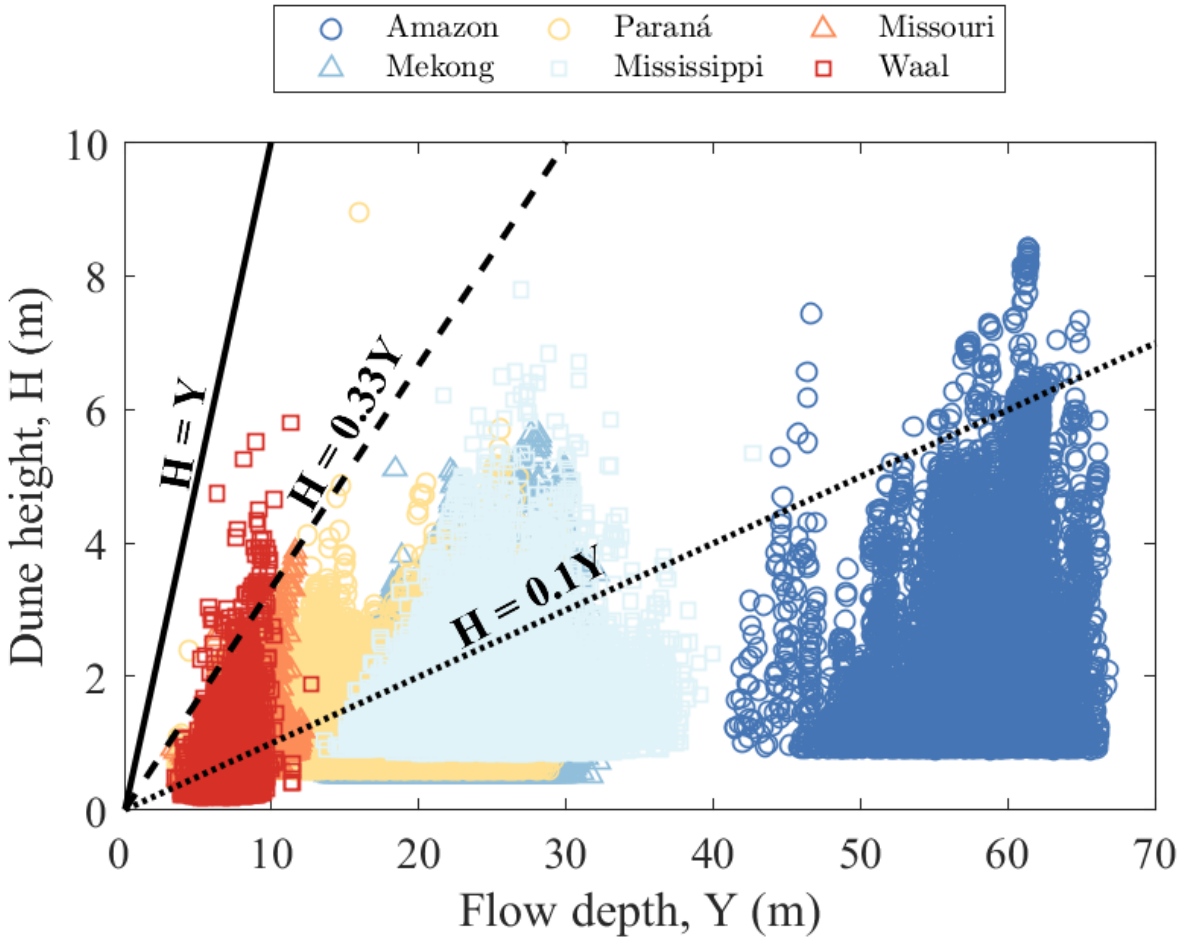

Figure 3. Flow depth vs dune height for dunes in all rivers.

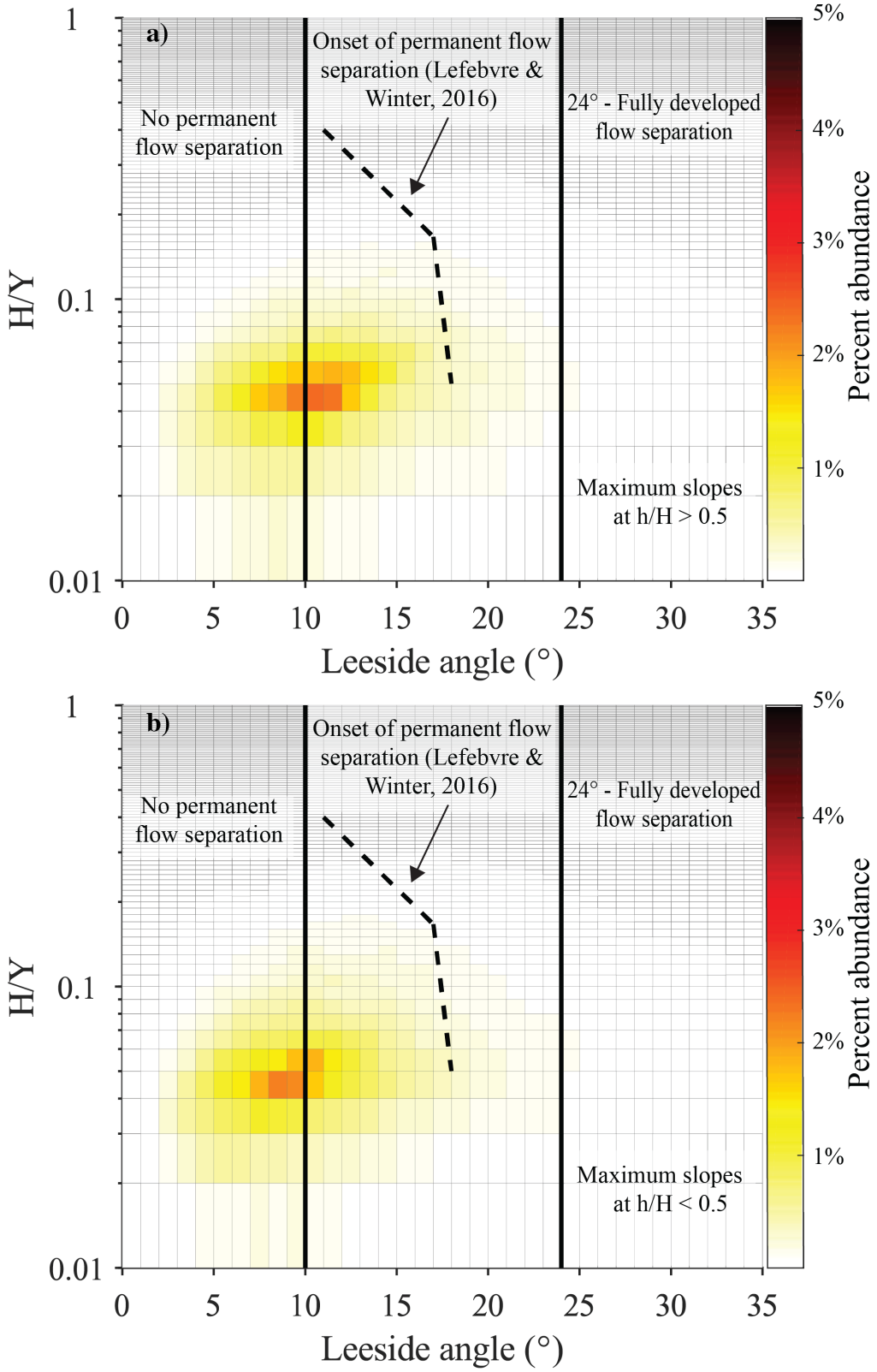

Figure 4. Hot spot graph (2D histogram) showing the potential for flow separation represented as a function of the submerged dune height (H/Y), leeside angle, and fractional height of the leeside maximum slope, with zones of no permanent flow separation, the onset of flow separation and fully developed flow separation[27]. a) Maximum leesides located on the top half of the dune leeside and b) in the bottom half of the dune leeside. 2D bin units are 0.01 H/Y and 1°.

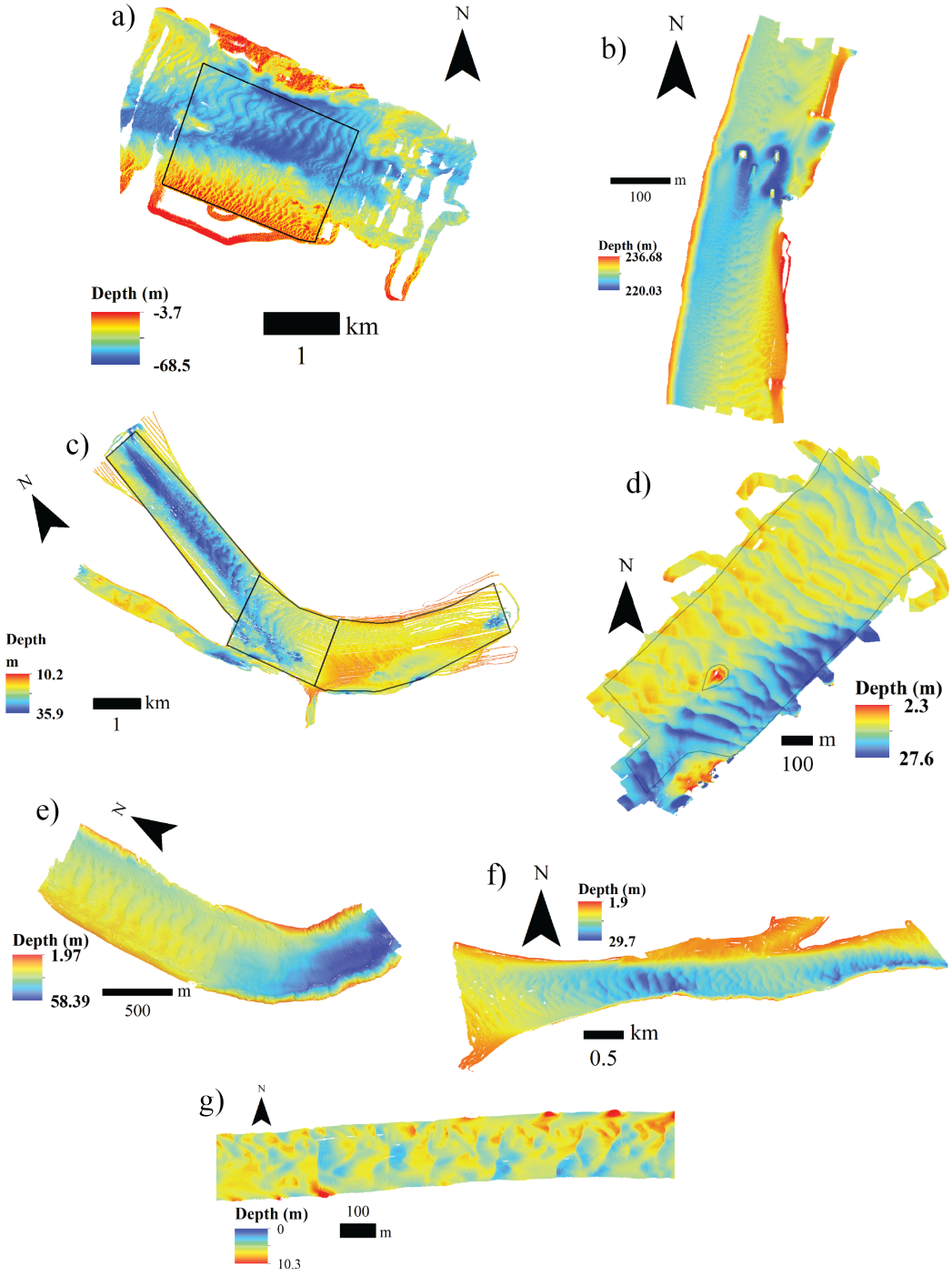

Figure S1. Multi-beam echosounder (MBES) maps of rivers analysed in this study from six rivers: a) Amazon, Brazil; b) Mekong, Cambodia; c) Mississippi, USA; d) Missouri, USA; e) Paraná near Paso de la Patria, Argentina; f) Paraná near Aguas Corrientes, Argentina; g) Waal, Netherlands.

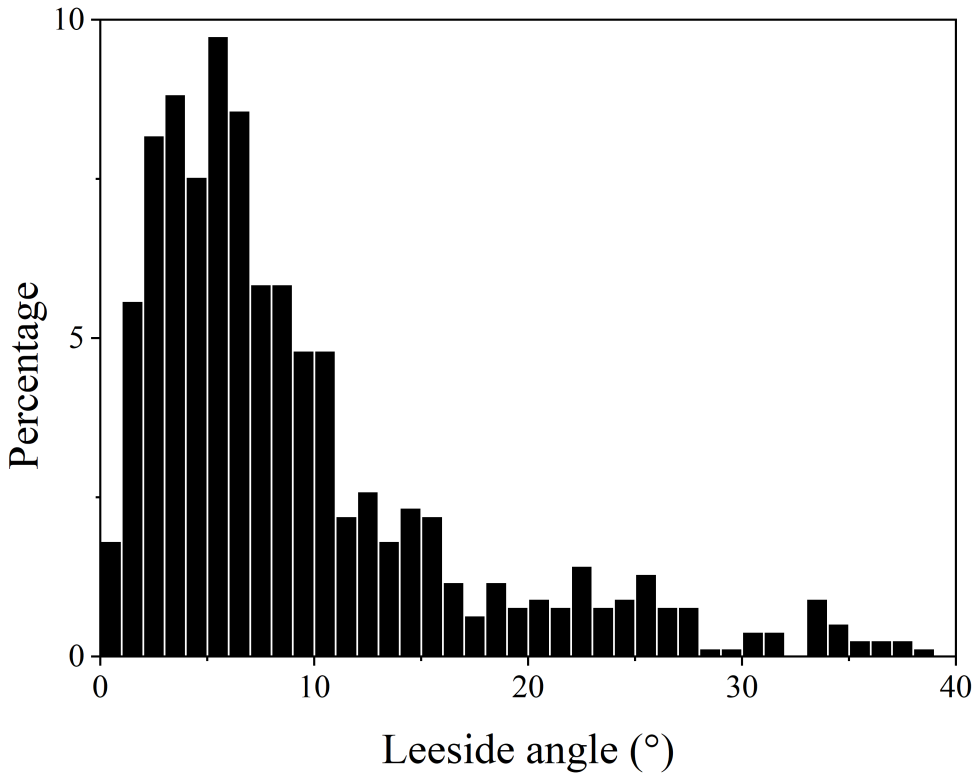

Figure S2. Distribution of mean dune leeside angles in the Jamuna (Brahmaputra) River (data from[18]).

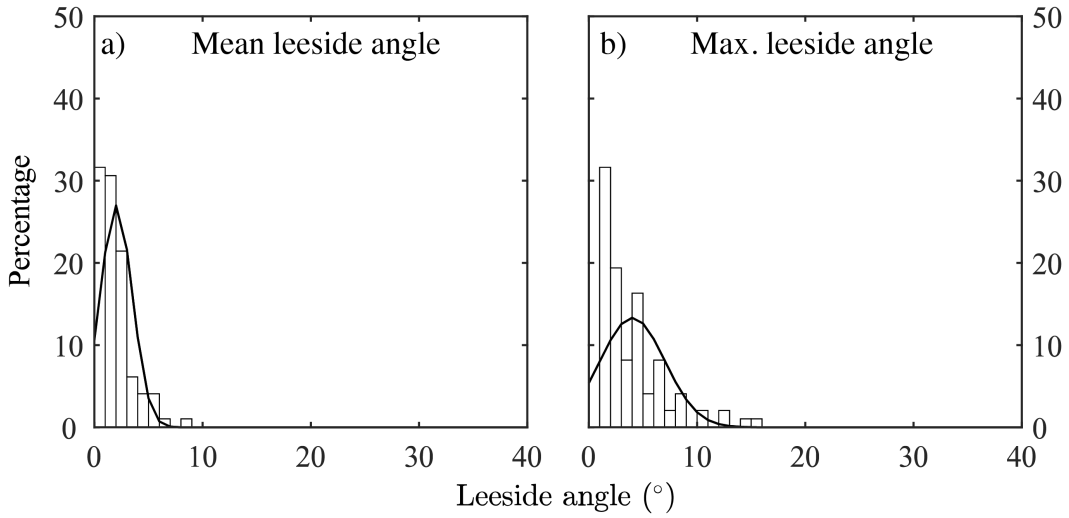

Figure S3. Distribution of mean and maximum dune leeside angles in the Huang He (Yellow) River. Leeside measurements were acquired using the BAMBI method from single echosounder lines.

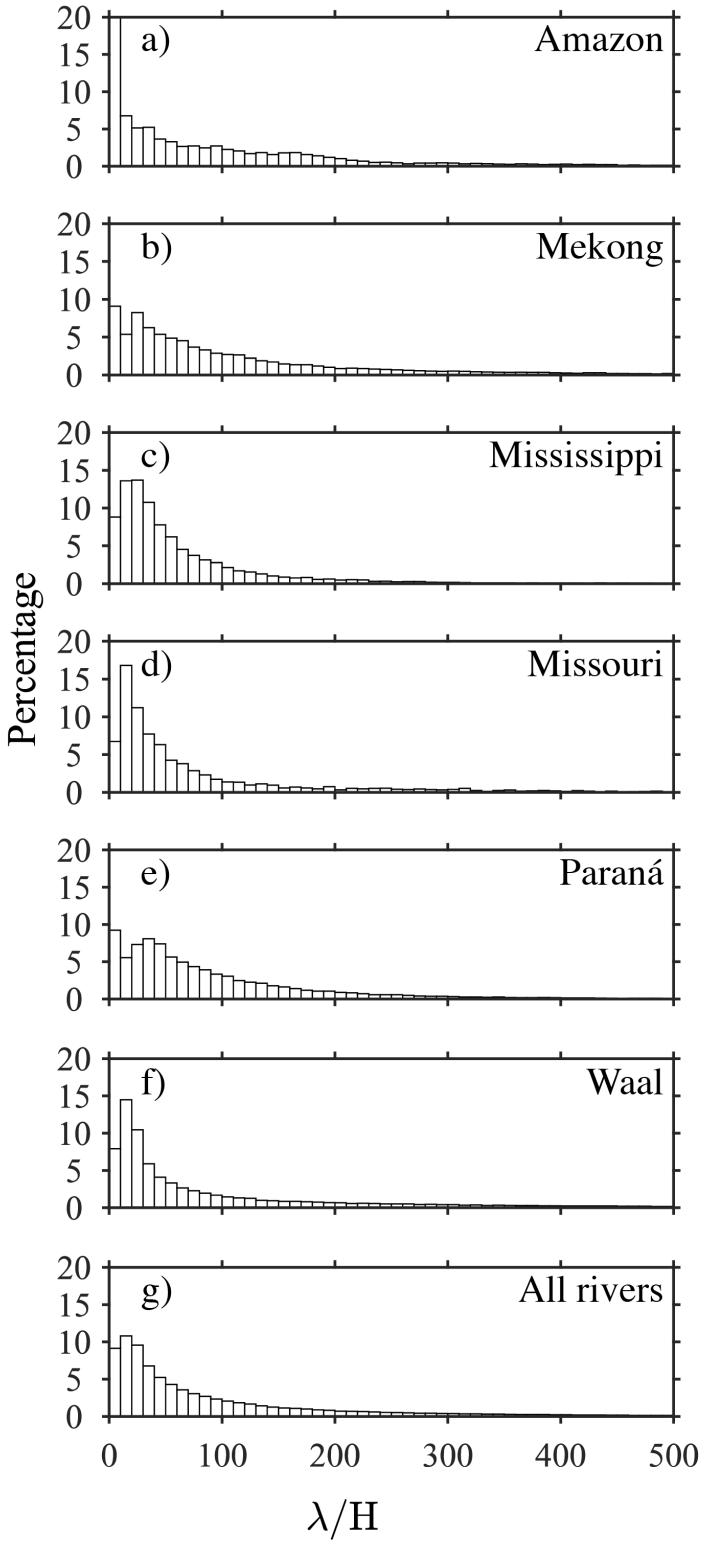

Figure S4. Distribution of dune aspect ratio (λ/H) for all rivers.

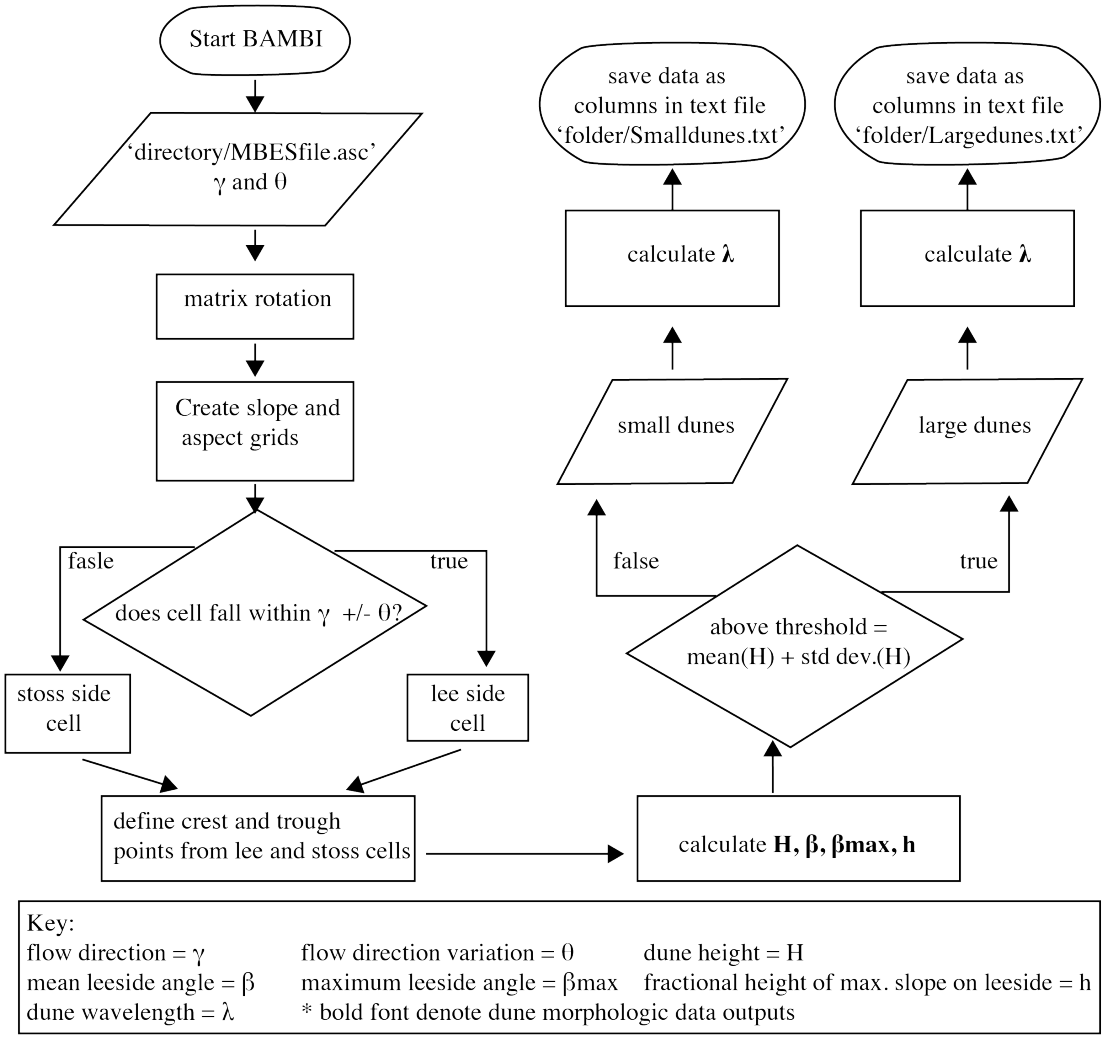

Figure S5. Flow chart illustrating the BAMBI methodology.